JOURNAL OF PETROLOGY | VOLUME 43 | NUMBER 11 | PAGES 2121–2142 | 2002

# Fluid-absent Melting of High-grade Semi-pelites: *P–T* Constraints on Orthopyroxene Formation and Implications for Granulite Genesis

**RAJEEV NAIR* AND THOMAS CHACKO**

DEPARTMENT OF EARTH AND ATMOSPHERIC SCIENCES, UNIVERSITY OF ALBERTA, EDMONTON, ALBERTA, CANADA T6G 2E3

**RECEIVED FEBRUARY 12, 2001; REVISED TYPESCRIPT ACCEPTED MAY 20, 2002**

*Rocks of semi-pelitic composition are common in high-grade terranes. The first appearance of orthopyroxene in these rocks marks the transition from amphibolite- to granulite-facies conditions, and is commonly attributed to the process of fluid-absent partial melting. We have conducted fluid-absent melting experiments on two natural semi-pelitic rocks (quartz, plagioclase, alkali feldspar, biotite and garnet) with the specific objective of determining the pressure–temperature conditions necessary to produce orthopyroxene. In contrast to previous experimental studies, our starting materials were obtained from a transitional amphibolite–granulite terrane. Importantly, the high $TiO_2$ (>5 wt %) and F (>1 wt %) contents of biotite in our experiments are more representative of biotite found in rocks on the verge of granulite-facies conditions than those used in earlier studies. Experiments were conducted in a piston-cylinder apparatus at 800–1050°C and 7–15 kbar. We reversed the first appearance of orthopyroxene in two-stage experiments at 7 and 10 kbar. Fluid-absent melting of biotite began at ~875°C with the production of a garnet–alkali-feldspar-bearing assemblage, and progressed with rising temperature to the generation of a garnet–orthopyroxene–alkali-feldspar-bearing assemblage. The initiation of the orthopyroxene-forming reaction, biotite + plagioclase + quartz = orthopyroxene + garnet + K-feldspar + melt, was bracketed between 925 and 950°C at 7 kbar, and at 1025 and 1050°C at 10 kbar. At pressures >10 kbar, orthopyroxene appeared at temperatures below 1035°C, suggesting a steepening and possibly a back-bend in the slope of the reaction. Our results indicate that temperatures of at least 875–1025°C are required to stabilize orthopyroxene under fluid-absent conditions at mid- to lower-crustal depths (5–15 kbar). This estimate is 40–120°C higher than reported in previous experimental studies on rocks of similar bulk composition. We attribute the difference to the higher Ti and F content of biotite in our starting materials, which stabilizes it to higher temperatures. The temperatures of fluid-absent orthopyroxene formation indicated by our experiments are also much higher than the 700–800°C temperatures reported for many orthopyroxene-bearing assemblages in amphibolite–granulite transitional terranes. One explanation for this discrepancy is that the geothermometers used to calculate temperatures for these transitional terranes grossly underestimated peak metamorphic temperatures. Alternatively, granulite formation in some of those terranes may not have been fluid absent, but involved the influx of low water activity fluids.*

KEY WORDS: *biotite; fluid-absent melting; granulite; metasediments; orthopyroxene*

## INTRODUCTION

Fluid-absent partial melting is widely held to be the dominant process responsible for stabilizing granulite-facies mineral assemblages in the deep continental crust (Fyfe, 1973; Clemens, 1992; Clemens *et al.*, 1997). This process has been investigated in a number of experimental studies (e.g. Le Breton & Thompson, 1988; Vielzeuf & Holloway, 1988; Patiño Douce & Johnston, 1991; Skjerlie & Johnston, 1993; Skjerlie *et al.*, 1993; Vielzeuf & Montel, 1994; Patiño Douce & Beard, 1995, 1996; Stevens *et al.*,

*Corresponding author. Telephone: 780-492-5395. Fax: 780-492-2030. E-mail: rajeev@ualberta.ca

1997; Patiño Douce & Harris, 1998; Pickering & Johnston, 1998), the majority of which were aimed at determining the fertility (melt productivity) of common crustal rock types or the composition of the melts generated from such rocks. Although these studies provided the general topology of the fluid-absent solidus for typical crustal rocks, very few specifically investigated the pressure–temperature conditions required for the formation of metamorphically significant anhydrous phases during the melting process. In particular, the appearance of orthopyroxene (opx) at the expense of hydrous minerals, biotite and/or hornblende marks the transition from amphibolite- to granulite-facies conditions. Quantification of the $P$–$T$ conditions at which opx first appears would enhance our understanding of the granulite-forming process and also provide a phase equilibrium constraint that is directly applicable in the field. The main objective of this study is to determine the $P$–$T$ conditions required for opx formation in semi-pelitic rocks by the process of fluid-absent melting.

The rationale for the present study stems from observations made regarding the composition of hydrous minerals in rocks undergoing amphibolite- to granulite-facies transition. Being dependent on the release of water stored in hydrous phases, the fluid-absent melting process is essentially a measure of the stability of hydrous phase(s) under fluid-absent conditions. Therefore, any compositional variable that affects the stability of these phases may affect the $P$–$T$ position of fluid-absent melting reactions. Two elements known to stabilize biotite to higher temperature are Ti and F (Forbes & Flower, 1974; Trønnes *et al.*, 1985; Peterson *et al.*, 1991; Patiño Douce, 1993; Dooley & Patiño Douce, 1996). Figure 1a compares the Ti content and Mg-number [molar Mg/(Mg + Fe)] of biotites from several transitional amphibolite–granulite terranes with those used in previous experimental melting studies on pelitic and semi-pelitic bulk compositions. The figure illustrates the Ti-rich nature of transitional terrane biotites compared with those used in previous melting experiments. Transitional terrane biotites are also generally higher in F than those used in previous experimental studies (Fig. 1b). Given these observations, it is possible that biotites from transitional terranes are stable to higher temperatures than indicated by earlier experiments.

The disparity between experimental and natural biotite compositions described above reflects the fact that the starting materials used in earlier experimental studies were taken from (or have mineral compositions typical of) mid- to upper-amphibolite-facies terranes rather than transitional amphibolite–granulite terranes. Thus, the compositions of these starting biotites do not represent equilibrium biotite compositions at transitional amphibolite–granulite $P$–$T$ conditions. Specifically, the biotites have not become enriched in Ti through high-temperature equilibration with Ti-saturating phases such as ilmenite or rutile (Patiño Douce, 1993), or enriched in F through the progress of sub-granulite melting reactions (e.g. muscovite + quartz breakdown). We suggest that an experimental study using rocks from transitional terranes as starting material would more closely simulate the fluid-absent melting process occurring in nature and thereby provide a better understanding of phase relations under high-grade conditions. In this paper, we present results of fluid-absent melting experiments on two high-grade semi-pelitic rocks, focusing on the $P$–$T$ conditions required for the first appearance of opx in these rocks. We also consider the implications of our experimental results for existing models of granulite genesis.

## METHODS

### Starting materials

In accord with the above arguments, the starting materials for the present experiments were rocks known from field relations to have been metamorphosed to near granulite-facies conditions. The starting materials were obtained from two localities, Ponmudi (PON) and Kalanjur (KAL), from the high-grade metasedimentary terrane of south India known as the Kerala Khondalite Belt (KKB). The KKB is dominated by garnet–biotite ± opx ± graphite gneisses (semi-pelites), and garnet–biotite–sillimanite–K-feldspar ± cordierite gneisses (pelites), intercalated with minor amounts of mafic granulites, calc-silicates and quartzites (Chacko *et al.*, 1987, 1992). These mineral assemblages indicate uppermost amphibolite- to granulite-facies metamorphic conditions throughout the KKB. PON and KAL are two of the many localities in the KKB that record the nature of the granulite-forming process. At these localities, granulite is developed as patches and veins that partially overprint the fabric of the host garnet–biotite gneiss (Fig. 2) (Ravindra Kumar *et al.*, 1985; Srikantappa *et al.*, 1985; Ravindra Kumar & Chacko, 1986). The gneissic and granulitic portions of the outcrop are virtually identical in their major-element compositions but differ mineralogically in that the granulite contains opx and significantly less biotite than the gneiss (Ravindra Kumar & Chacko, 1986). These mineralogical, geochemical and field relationships strongly suggest that garnet–biotite gneiss was the lithological precursor to the granulite. Moreover, the intimate spatial association of the two rock types requires that they were metamorphosed at very similar $P$–$T$ conditions, and specifically $P$–$T$ conditions that verged on those necessary to produce granulite-facies mineral assemblages. The opx-free gneiss at these localities would, therefore, serve as ideal starting material for investigating $P$–$T$ conditions of opx formation by fluid-absent melting of high-grade rocks.

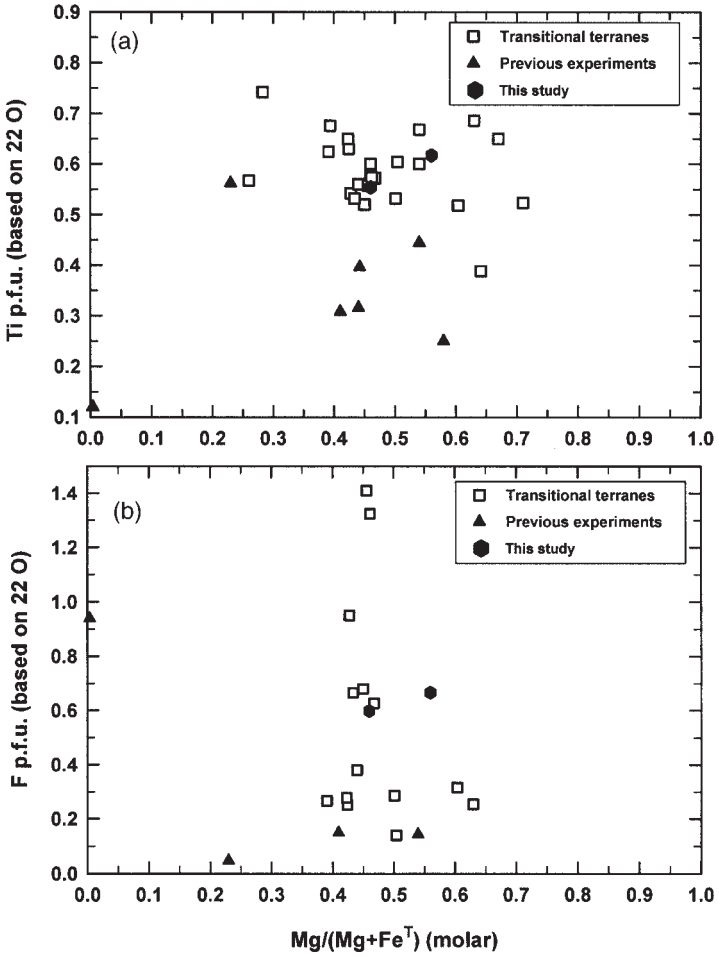


**Fig. 1.** Comparison of biotite compositions from amphibolite–granulite transitional terranes with those used in previous experimental studies. (a) Ti (per formula unit) vs Mg/(Mg + $Fe^T$). (b) F vs Mg/(Mg + $Fe^T$). Transitional terrane data sources: South India, Janardhan *et al.* (1982) and Hansen *et al.* (1987); Sri Lanka, Hansen *et al.* (1987) and Burton & O'Nions (1990); Antarctica, Santosh & Yoshida (1992); Uusimaa, Finland, Schreurs (1985); Seiland Province, Norway, Elvevold *et al.* (1994); Ivrea Zone, Italy, Franz & Harlov (1998); Wayah, USA, Eckert *et al.* (1989); Reading Prong, USA, Young (1995); Wyoming, USA, Grant & Frost (1990); Quetico subprovince, Canada, Pan *et al.* (1994); Slave Province, Canada, T. Chacko (unpublished data, 1997). Experimental biotites: Le Breton & Thompson (1988), Patiño Douce & Johnston (1991), Vielzeuf & Montel (1994), Patiño Douce & Beard (1995, 1996) and Stevens *et al.* (1997).

The bulk-rock and mineralogical compositions of the starting materials are given in Table 1. Both starting materials contain the mineral assemblage biotite–quartz–plagioclase–K-feldspar–garnet–ilmenite and have whole-rock compositions broadly corresponding to those of metagraywackes. The two rocks differ in that biotite in KAL is more magnesian and slightly more Ti- and F-rich than biotite in PON. Additionally, graphite has been reported in the Ponmudi quarry (Ravindra Kumar *et al.*, 1985), and may be present in trace quantities in the PON starting material, whereas it is absent from the Kalanjur quarry (Ravindra Kumar & Chacko, 1986) and the KAL starting material. As shown in Fig. 1, the biotite of the present starting materials has higher Ti and F content than those of previous experimental studies. The modal compositions of both starting materials are such that biotite is the phase that limits melt production under fluid-absent conditions.

## Experimental procedures

All experiments were performed under fluid-absent conditions in an end-loaded piston-cylinder apparatus using a piston of 1·91 cm (3/4 inch) diameter. The sample assembly, of 4·4 cm length, consisted of an outer NaCl sleeve and an inner Pyrex glass sleeve containing a tapered graphite furnace (Kushiro, 1976) and crushable

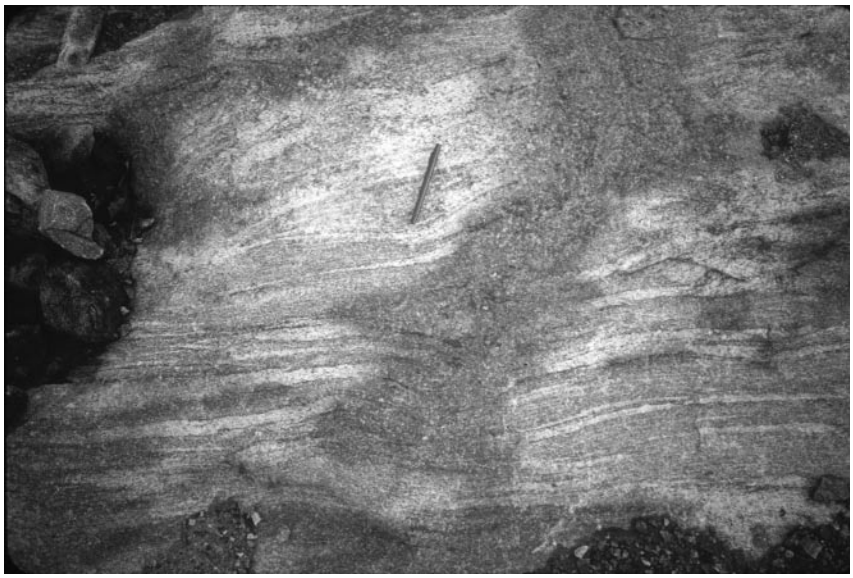

**Fig. 2.** Close view of incipient granulite patch (dark) transecting garnet–biotite gneiss (light colored) at Ponmudi. The obliteration of the gneissic foliation against the granulite patch should be noted. The foliation, however, is faintly preserved in some areas within the granulite. Starting material for the present experiments was taken from the light-colored gneissic portion of the outcrop.

ceramic inner parts. The experimental capsules were placed in a ceramic inner sleeve near the center of the graphite furnace. Any free space between the ceramic sleeve and the capsules was filled with Pyrex powder. The NaCl outer sleeve was fired at 300–350°C for ~1 h before use in the experiments. The sample assembly was jacketed with Pb foil to minimize friction between the assembly and the pressure vessel.

Nominal hydraulic pressures were measured with a Heise bourdon tube gauge and converted to sample pressure using a theoretically calculated pressure amplification factor. Correspondence between calculated and true sample pressures was evaluated using the equilibrium Grossular + Quartz = Wollastonite + Anorthite, relative to the *P–T* position of this equilibrium reported by Windom & Boettcher (1976) and Mattioli & Bishop (1984). These calibration experiments indicated that no pressure correction is required with this sample assembly. The reported pressures are believed to be accurate to within 500 bar. Temperatures were measured with $W_5Re$–$W_{26}Re$ thermocouples, and controlled to within ±5°C of the set point. The reported temperatures are considered to be accurate within 10°C.

For each experiment, the samples were cold pressurized to 2–3 kbar above the desired pressure, and the temperature then manually raised to the desired experimental temperature over a 10–15 min period. The final experimental conditions were always attained by release of pressure (hot, piston-out technique). Experiments were quenched by cutting off power to the furnace, which cooled samples to below 600°C in about 5 s.

In addition to the single-step experiments, phase reversal experiments involving a two-step procedure were carried out. In the first step, the starting materials were equilibrated at the *P–T* conditions where the appearance of the phase of interest (opx) was documented in a previous single-step experiment. During the second step, the temperature of the experiment was lowered while keeping the pressure constant. The criteria for successful reversal include the disappearance of opx and the growth of euhedral biotite crystals. The reversal biotites had compositions similar to those found in lower-temperature single-step experiments.

The starting materials were ground in an agate mortar with distilled water to an average grain size of <10 μm. The powdered material was then treated with dilute HCl to leach away any retrograde chlorite that may have been present in the sample. The samples were rinsed thoroughly with distilled water after the acid treatment and stored in an oven at 120°C for several days before loading the capsules.

Approximately 10–15 mg of starting material was loaded into gold capsules of 2 mm o.d. Two capsules were run in each experiment, one containing the PON and the other the KAL starting material. Considerable care was taken to minimize $H_2O$ adsorption on the rock powders during the loading process. This includes storing the loaded and partially crimped capsules in a 120°C oven for at least 15 h before final crimping inside the oven and immediate arc welding. The capsules were weighed before and after each experiment and those with any tear and/or weight loss >0·1 mg were discarded.

*Table 1: Composition of starting materials*

| wt %: | $SiO_2$ | $TiO_2$ | $Al_2O_3$ | $FeO^T$ | MnO | MgO | CaO | $Na_2O$ | $K_2O$ | F | Cl | Total | Modal % | Mg-no.* |
|---|---|---|---|---|---|---|---|---|---|---|---|---|---|---|
| *Ponmudi* | | | | | | | | | | | | | | |
| Biotite | 37·58 | 5·02 | 13·76 | 21·88 | 0·03 | 10·62 | 0·01 | 0·12 | 10·21 | 1·26 | 0·32 | 100·81 | 10 | 46 |
| Plagioclase | 59·31 | n.a. | 24·68 | 0·03 | 0·01 | 0·00 | 6·61 | 7·66 | 0·27 | n.a. | n.a. | 98·57 | 28 | |
| K-feldspar | 64·87 | 0·02 | 18·73 | 0·01 | 0·00 | 0·00 | 0·14 | 1·63 | 14·04 | n.a. | n.a. | 99·44 | 14 | |
| Garnet | 37·20 | 0·05 | 21·29 | 34·85 | 0·68 | 3·69 | 2·53 | 0·00 | n.a. | n.a. | n.a | 100·29 | 16 | 16 |
| Ilmenite | 0·01 | 52·30 | n.a. | 47·63 | 0·07 | 0·03 | 0·03 | n.a. | n.a. | n.a. | n.a. | 100·07 | <2 | |
| Quartz | n.a. | n.a. | n.a. | n.a. | n.a. | n.a. | n.a. | n.a. | n.a. | n.a. | n.a. | | 30 | |
| *Kalanjur* | | | | | | | | | | | | | | |
| Biotite | 35·87 | 5·45 | 13·62 | 17·38 | 0·02 | 12·63 | 0·01 | 0·11 | 9·60 | 1·40 | 0·35 | 96·44 | 11 | 56 |
| Plagioclase | 58·25 | n.a. | 25·49 | 0·03 | 0·01 | 0·01 | 7·63 | 7·03 | 0·24 | n.a. | n.a. | 98·69 | 30 | |
| K-feldspar | 64·66 | 0·05 | 18·99 | 0·01 | 0·01 | 0·00 | 0·37 | 2·22 | 12·91 | n.a. | n.a. | 99·22 | 10 | |
| Garnet | 37·73 | 0·04 | 21·73 | 32·40 | 0·67 | 6·13 | 1·81 | 0·01 | n.a. | n.a. | n.a. | 100·54 | 18 | 25 |
| Ilmenite | 0·03 | 52·30 | n.a. | 46·15 | 0·19 | 0·02 | 0·02 | n.a. | n.a. | n.a. | n.a. | 98·69 | <1 | |
| Quartz | n.a. | n.a. | n.a. | n.a. | n.a. | n.a. | n.a. | n.a. | n.a. | n.a. | n.a. | | 30 | |
| *Bulk composition† (wt %)* | | | | | | | | | | | | | A/CNK‡ | |
| Ponmudi | 68·80 | 0·83 | 14·60 | 5·99 | 0·08 | 1·05 | 2·13 | 2·55 | 4·42 | n.a. | n.a. | 100·45 | 1·15 | 23 |
| Kalanjur | 68·00 | 0·94 | 14·40 | 6·22 | 0·11 | 1·56 | 2·45 | 2·40 | 3·63 | n.a. | n.a. | 99·71 | 1·18 | 31 |

*Molar $(Mg/Fe^T + Mg) \times 100$. †From Chacko (1987). ‡Molar $[Al_2O_3/(CaO + Na_2O + K_2O)]$.
T, total Fe reported as FeO; n.a., not analyzed.

Experiments were conducted at temperatures from 800°C to 1000°C at 7 kbar, 875°C to 1050°C at 10 kbar, and 950°C to 1050°C at 15 kbar. Run duration varied from 3 weeks at 800°C to 2 days at 1050°C. The duration of experiments was kept short at high temperatures (>900°C) to minimize any possible desiccation of the samples through diffusion of volatiles through the capsule walls (Patiño Douce & Beard, 1994).

### Analytical procedures

The run products were mounted in epoxy and analyzed using energy-dispersive (EDS) and wavelength-dispersive (WDS) modes with a JEOL 8900 electron microprobe at the University of Alberta. The proportions of the phases were estimated from backscattered electron images. WDS analyses were performed at an accelerating voltage of 15 kV, a beam current of 15 nA, and a beam diameter between 1 and 3 μm. Natural minerals were used as standards for all the phases. X-ray counts were converted to concentrations by means of a ZAF correction routine. The melt pockets in the run products were often too small (<2 μm wide) to obtain reliable analyses. However, a few representative analyses of the glass were made using a beam diameter of 1 μm. At these conditions, migration of alkalis during glass analyses is known to be a significant problem. To minimize this problem, Na and K were analyzed first and the counting time for Na was limited to 10 s. Although the small size of the melt pockets precluded monitoring of count-rate decay of Na and K with time, some alkali migration undoubtedly took place during the analyses. Therefore, all melt compositions reported here should be taken as approximations. We note, however, that analytical totals and alkali contents for the melts in our experiments are similar to those reported for melts in other experimental studies on comparable bulk compositions. Problems were also encountered in analyzing opx because of the small (1–3 μm) width of most opx crystals. Thus, even focused beam analyses incorporated small amounts of surrounding ilmenite, and/or melt, as is evident in the elevated $TiO_2$ and $K_2O$ content of the analyses. The analyses were corrected assuming all K in opx represents glass contamination.

### Redox conditions

No external oxygen buffers were used in the experiments. However, oxygen fugacity was calculated for all experimental products that contained opx, ilmenite and quartz with the equilibrium $2Fe_2O_3 + 4SiO_2 = 2Fe_2Si_2O_6 + O_2$. One set of calculations used the standard state properties of Berman (1988) for end-member phases, and the solution properties of Sack & Ghiorso (1989) and Ghiorso (1990) for opx and ilmenite, respectively, whereas a second set of calculations used the QUIlF program (Anderson *et al.*, 1993). Calculated oxygen fugacities generally range from one-half to two log units below that of the quartz–fayalite–magnetite (QFM) buffer (Table 2), which is typical for experiments using piston-cylinder assemblies similar to that employed in the present study (Patiño Douce & Beard, 1995, 1996). The similarity in oxygen fugacities facilitates comparison between our results and those of earlier studies.

## RESULTS

### Description of the run products

*7 kbar*

Trace amounts of melt were observed in the run products of PON and KAL at 800°C, the lowest temperature investigated at this pressure (Table 2). The amount of biotite in the run products decreased from ~10% at 800°C to <1% at 1000°C. This corresponds to an increase in the proportion of garnet, alkali feldspar and melt, and a decrease in the proportion of plagioclase and quartz for the same temperature range. Although melting began at <800°C, opx did not appear as a stable phase until >925°C, where its appearance was reversed in both KAL and PON. The ferromagnesian silicate phases stable until the appearance of opx in both starting materials are biotite, garnet and melt. Ilmenite was the only oxide phase present.

*10 kbar*

Melting occurred in all the runs conducted at 10 kbar in both KAL and PON. The abundance of biotite at any temperature is higher than that in the corresponding 7 kbar experiment. Plagioclase is less abundant and garnet more abundant than in the lower-pressure experiments. The presence of opx was reversed between 1025 and 1050°C. In the single-step experiments, opx was observed only at 1050°C, where it occurs as needles and prisms pseudomorphing biotite. Disappearance of opx in the reversal experiment corresponds to the growth of euhedral grains of biotite, as was observed in the reversal experiment at 7 kbar. In addition to ilmenite, rutile is present in some 10 kbar experiments.

*12·5 kbar*

A single experiment at 1035°C contained garnet as the dominant mafic product phase with subordinate amounts of opx in both samples. Opx occurs as small prismatic crystals in PON in contact with neoblastic euhedral garnets. In KAL opx also forms large crystals pseudomorphing biotite. Biotite is absent in both samples. The proportion of the melt is greater than that in the 1000°C

*Table 2: Experimental conditions and mineral assemblage*

| Run no. | *P* (kbar) | *T* (°C) | Duration (h) | $f(O_2)$ Δlog QFM* | Mineral assemblage |
|---|---|---|---|---|---|
| *Ponmudi* | | | | | |
| RJ-05 | 7 | 800 | 504 | | Bio, Grt, Plg, Kfs, Qtz, Ilm, Py, M |
| RJ-03 | 7 | 850 | 336 | | Bio, Grt, Plg, Kfs, Qtz, Ilm, M |
| RJ-33 | 7 | 875 | 336 | | Bio, Grt, Plg, Kfs, Qtz, Ilm, M |
| RJ-11 | 7 | 900 | 336 | | Bio, Grt, Plg, Kfs, Qtz, Ilm, M |
| RJ-09 | 7 | 950 | 168 | −1·61 | Bio, Grt, Opx, Plg, Kfs, Qtz, Ilm, M |
| RJ-25 | 7 | 1000 | 48 | −0·41 | (Bio), Grt, Opx, Plg, Kfs, Qtz, Ilm, M |
| RJ-27 | 7 | 1000 | 48 | | |
| → | 7 | 925 | 168 | | Bio, Grt, Plg, Kfs, Qtz, Ilm, M |
| RJ-17 | 10 | 875 | 336 | | Bio, Grt, Plg, Kfs, Qtz, Ilm, Py, M |
| RJ-15 | 10 | 900 | 336 | | Bio, Grt, Plg, Kfs, Qtz, Ilm, Py, Ru, M |
| RJ-13 | 10 | 950 | 168 | | Bio, Grt, Plg, Kfs, Qtz, Ilm, Ru, M |
| RJ-23 | 10 | 1000 | 168 | | Bio, Grt, Plg, Kfs, Qtz, Ilm, M |
| RJ-31 | 10 | 1050 | 48 | −1·58 | Grt, Plg, Opx, Kfs, Qtz, Ilm, Ru, M |
| RJ-35 | 10 | 1050 | 48 | | |
| → | 10 | 1025 | 48 | | Bio, Grt, Plg, Kfs, Qtz, Ilm, M |
| RJ-39 | 12·5 | 1035 | 72 | | Grt, Kfs, Plg, Qtz, Opx, Ilm, M |
| RJ-19 | 15 | 950 | 240 | | Bio, Grt, Plg, Kfs, Qtz, Ilm, Ru, Py, M |
| RJ-21 | 15 | 1000 | 96 | | Bio, Grt, Plg, Opx, Kfs, Qtz, Ru, M |
| RJ-29 | 15 | 1050 | 48 | | Grt, Plg, Kfs, Qtz, Ru, M |
| RJ-37 | 15 | 1050 | 48 | | |
| → | 15 | 975 | 72 | | Bio, Grt, Plg, Kfs, Qtz, Ilm, M |
| *Kalanjur* | | | | | |
| RJ-06 | 7 | 800 | 504 | | Bio, Grt, Plg, Kfs, Qtz, Ilm, Py, M |
| RJ-04 | 7 | 850 | 336 | | Bio, Grt, Plg, Kfs, Qtz, Ilm, Py, M |
| RJ-34 | 7 | 875 | 336 | | Bio, Grt, Plg, Kfs, Qtz, Ilm, M |
| RJ-12 | 7 | 900 | 336 | | Bio, Grt, Plg, Kfs, Qtz, Ilm, M |
| RJ-10 | 7 | 950 | 168 | −2·22 | Bio, Grt, Opx, Plg, Kfs, Qtz, Ilm, M |
| RJ-26 | 7 | 1000 | 48 | −0·28 | (Bio), Grt, Opx, Plg, Kfs, Qtz, Ilm, M |
| RJ-28 | 7 | 1000 | 48 | | |
| → | 7 | 925 | 168 | | Bio, Grt, Plg, Kfs, Qtz, Ilm, M |
| RJ-18 | 10 | 875 | 336 | | Bio, Grt, Plg, Kfs, Qtz, Ru, M |
| RJ-16 | 10 | 900 | 336 | | Bio, Grt, Plg, Kfs, Qtz, Ilm, M |
| RJ-14 | 10 | 950 | 168 | | Bio, Grt, Plg, Kfs, Qtz, Ilm, M |
| RJ-24 | 10 | 1000 | 168 | | Bio, Grt, Plg, Kfs, Qtz, Ilm, M |
| RJ-32 | 10 | 1050 | 48 | −2·41 | (Bio), Grt, Opx, Plg, Kfs, Qtz, Ilm, M |
| RJ-36 | 10 | 1050 | 48 | | |
| → | 10 | 1025 | 48 | | Bio, Grt, Plg, Kfs, Qtz, Ilm, M |
| RJ-40 | 12·5 | 1035 | 72 | | Grt, Kfs, Plg, Qtz, Opx, Ilm, M |
| RJ-20 | 15 | 950 | 240 | | Bio, Grt, Plg, Kfs, Qtz, Ru, M |
| RJ-22 | 15 | 1000 | 96 | | Bio, Grt, Plg, Kfs, Qtz, Ru, M |
| RJ-30 | 15 | 1050 | 48 | | Grt, Plg, Kfs, Qtz, Ilm, M |
| RJ-38 | 15 | 1050 | 48 | | |
| → | 15 | 975 | 72 | | Bio, Grt, Plg, Kfs, Qtz, Ru, M |

*Oxygen fugacity calculated using QUIIF program (Anderson *et al.*, 1993).
→ indicates second step of the experiment. Bio, biotite; Grt, garnet; Plg, plagioclase; Kfs, alkali feldspar; Opx, orthopyroxene; Ilm, ilmenite; Ru, rutile; Py, pyrrhotite; M, quenched melt. Parentheses indicate that only trace amount of the phase was present.

run at 7 kbar in both samples. Plagioclase abundance is considerably less than that in the 7 kbar experiments. Ilmenite was the only oxide phase present.

*15 kbar*

At 950°C, the more friable nature of the run product compared with the corresponding 7 kbar experiment suggests that the proportion of melt is considerably less at 15 kbar. The melt proportion, however, increases substantially from 950°C to 1050°C. Garnet is more abundant than in any of the low-pressure experiments. Garnet grains exhibit zoning in all of the high-pressure runs, but the zoning is limited to the outer ~1–1·5 μm of the grains. In the 1050°C experiments the garnet crystals pseudomorph biotite. The proportion of plagioclase is considerably lower than in the low-pressure experiments. Opx is present in the 1000°C experiment with PON, but is absent from all the other experiments with PON, and from all experiments on KAL at 15 kbar. Biotite was absent from both KAL and PON samples at 1050°C. In a two-step experiment involving equilibration at 1050°C for 2 days and subsequent equilibration at 975°C for 3 days, opx was not observed as a phase in both KAL and PON. However, the run product showed growth of biotite as euhedral grains.

## Phase compositions

The full dataset of phase compositions may be downloaded from the *Journal of Petrology* web site at http://www.petrology.oupjournals.org.

*Biotite*

Biotite is a restite phase in experiments at 1000°C and below but is absent from all higher-temperature (>1000°C) experiments except for the run RJ-31 (1050°C, 10 kbar), which contains a few residual grains of the mineral. Biotite typically occurs as elongate (5–50 μm), ribbon-like grains with resorbed margins (Fig. 3a). In most run products, a thin film of quenched melt surrounds biotite grains. Small (<2 μm) grains of ilmenite and/or rutile commonly nucleate on or near biotite.

Biotite analyses with >39 wt % silica were discarded (because of possible silica contamination) and the rest were averaged for each run product. Biotite compositions vary with pressure and temperature in experiments with both PON and KAL. The most notable variations are overall increases in Mg-number, Ti and F with rising temperature (Figs 4 and 5). We attribute the increase in the Mg-number at temperatures above 875°C (Fig. 4a) to preferential breakdown of the annite and siderophyllite (Fe–Al) components in biotite to produce garnet, and at higher temperature, garnet and opx. These trends in biotite composition can be described by the following equilibria:

$$4KFe_3AlSi_3O_{10}(OH)_2 + 3[Al_2Fe_{-1}Si_{-1}]_{biotite} + 12SiO_2 = 4KAlSi_3O_8 + 3Fe_3Al_2Si_3O_{12} + 4[H_2O]_{melt}$$

$$2KFe_3AlSi_3O_{10}(OH)_2 + 6SiO_2 = 2KAlSi_3O_8 + 3Fe_2Si_2O_6 + 2[H_2O]_{melt}$$

$$[FeMg_{-1}]_{biotite} = [FeMg_{-1}]_{garnet} = [FeMg_{-1}]_{opx}.$$

Progress of the first two reactions, and partitioning of Fe into garnet and opx relative to biotite results in a residual biotite with higher Mg and lower Al than the starting biotite. This is evident from Fig. 4b, which shows that there is a general trend towards decreasing Al content with increasing Mg-number. The same fluid-absent melting reactions also cause an increase in the Ti and F content of the biotite because of the preferential consumption of hydroxy-annite and siderophyllite components of biotite in the reaction. The variations in the Ti and F content of biotites in our experiments can be described by the equilibria (Patiño Douce, 1993)

$$[Al_2Fe_{-3}]_{biotite} + 2FeTiO_3 + 3SiO_2 = 2[TiFe_{-2}]_{biotite} + Fe_3Al_2Si_3O_{12}$$

$$2FeTiO_3 + 6SiO_2 = 2[TiFe_{-2}]_{biotite} + 3Fe_2Si_2O_6$$

$$[FOH_{-1}]_{biotite} = [FOH_{-1}]_{melt}.$$

*Garnet*

Garnet is both a relict and a neoblastic phase in all the experiments. Newly grown garnet mostly nucleated as discrete grains, although growth also occurred on the rims of pre-existing garnet grains. Garnet neoblasts can be distinguished from relict grains by their euhedral shape and the presence, in some cases, of melt inclusions. The neoblasts commonly formed in the vicinity of relict biotite crystals with textures suggestive of formation through biotite breakdown. The abundance of garnet increases with pressure, with the largest increase between 10 and 15 kbar.

Garnet grains range in size from <1 to >15 μm. The composition of larger grains varies only slightly with changing pressure and temperature, suggesting that these grains did not equilibrate compositionally during the experiments. Smaller euhedral grains, however, do show compositional variation with changing pressure and temperature. The variation of garnet composition with temperature is shown in Fig. 6.

*Plagioclase*

Plagioclase is a common restitic phase in all the run products and ranges from <1 μm to >15 μm in diameter. It mostly occurs as anhedral grains and decreases in abundance with rising temperature, suggesting that it is

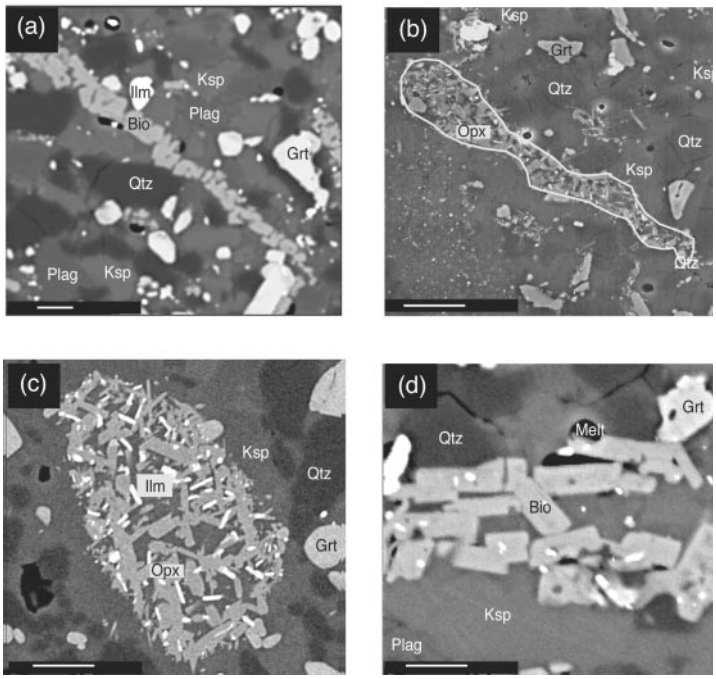


**Fig. 3.** Backscattered electron images of run products. (a) Typical morphology of biotite in single-step experiments in which melting occurred. The highly resorbed margins indicative of biotite breakdown should be noted. Also observable are euhedral garnets that have grown during the experiment. (b) Matted orthopyroxene crystals pseudomorphing biotite in the 7 kbar, 1000°C experiment on Ponmudi. (c) Prismatic crystals of orthopyroxene that grew in the 7 kbar, 1000°C experiment on Kalanjur. The tiny needles of ilmenite should also be noted. (d) Euhedral biotite crystals that grew in the reversal experiment at 7 kbar on Ponmudi. The euhedral biotite growth and the absence of orthopyroxene in these runs were used as criteria for a successful reversal of opx-in reaction. Scale bar in each image represents 5 μm.

a reactant phase in the melting reactions. Plagioclase compositions are uniform on an intra-grain as well as on intra-sample scale. Montel & Vielzeuf (1997) reported excess silica and/or Al in their plagioclase grains, but no indication of this non-stoichiometry was noted in the analyses of the present study. At constant pressure, the anorthite content increases with rising temperature (Fig. 7a). This reflects the preferential incorporation of the albite component of plagioclase into the melt leaving behind a more anorthitic plagioclase. There is also a consistent increase in the orthoclase content of plagioclase with rising temperature (Fig. 7), which is a consequence of the shrinkage of the ternary feldspar solvus with rising temperature. The plagioclase compositions generally plot within 50°C of the appropriate isotherm on the ternary feldspar solvus (Elkins & Grove, 1990). The small decrease in the orthoclase content of plagioclase with increasing pressure is consistent with expansion of the ternary feldspar solvus with pressure (Elkins & Grove, 1990).

### *Alkali feldspar*

Alkali feldspar is a common neoblastic phase in all experiments that produced melt. It occurs as homogeneous crystals, up to 10 μm in diameter, and commonly in contact with plagioclase grains. Some relict crystals are also present, but no compositional differences were detected between neoblastic and relict grains.

In contrast to the present experiments, alkali feldspar was not observed as a product of biotite fluid-absent melting in many previous studies (Vielzeuf & Holloway, 1988; Patiño Douce & Johnston, 1991; Vielzeuf & Montel, 1994; Patiño Douce & Beard, 1996). Patiño Douce & Beard (1995, 1996) attributed the absence of alkali feldspar in their run products to nucleation difficulties arising from limited temperature range over which melt and alkali feldspar coexist. Carrington & Watt (1995) proposed that the behavior of alkali feldspar during fluid-absent melting depends upon the relative $H_2O$:$K_2O$ ratio of melt and biotite, and that higher ratio in melt favors production of alkali feldspar during melting. The absence of alkali feldspar in some of the earlier studies could be attributed to the fact that it was not present in the starting material of those experiments. Therefore, any alkali feldspar component produced by biotite breakdown was incorporated as an orthoclase component in plagioclase or melt (Vielzeuf & Montel, 1994). In contrast, the presence of 10–15 modal % of alkali feldspar in the starting materials of the present experiments saturated melt and plagioclase at experimental conditions, and allowed preservation of neoblastic alkali feldspar.

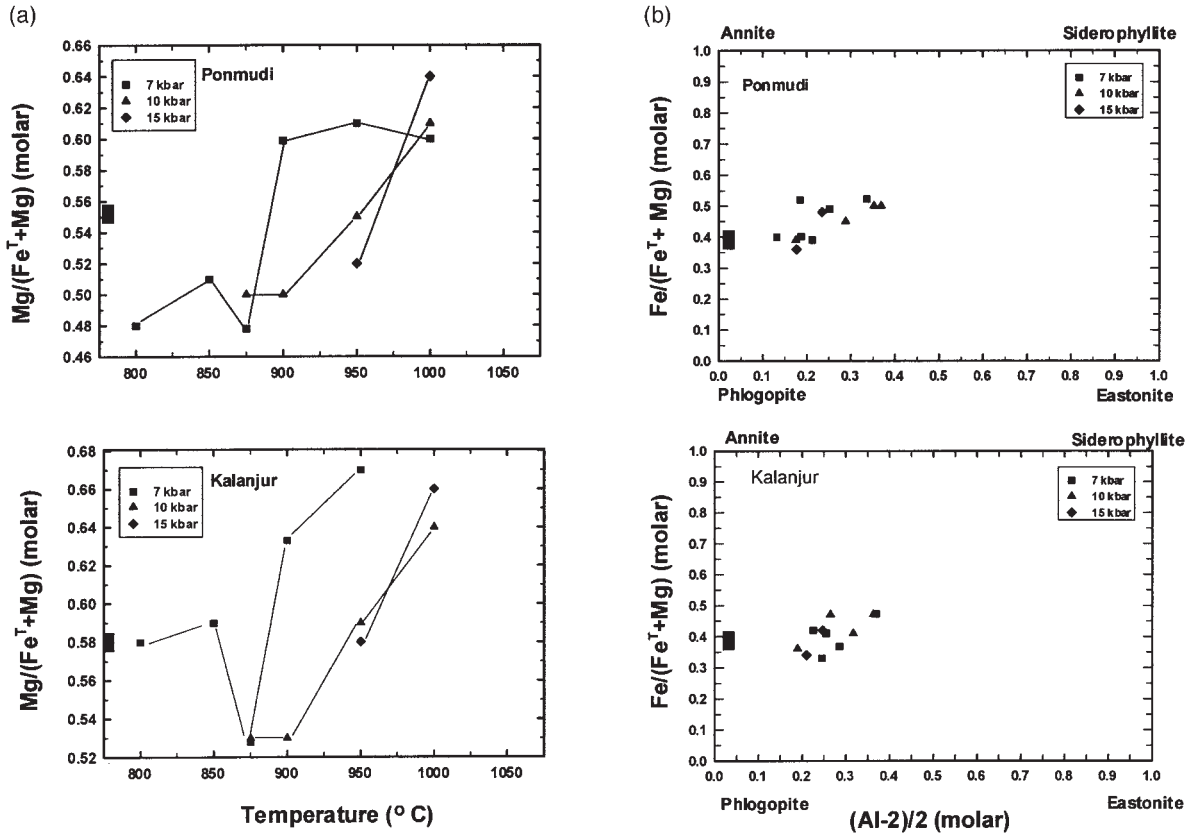


**Fig. 4.** Biotite compositions. (a) Molar Mg/(Mg + $Fe^T$) vs temperature. (b) Annite–eastonite diagram illustrating the variation of Al content with Fe/Mg ratio. Bars represent typical 1σ standard deviation of data in a single experiment.

The orthoclase content of alkali feldspar decreases with rising temperature whereas the anorthite and albite content increases (Fig. 8). This can be attributed to the increased solubility of plagioclase component in alkali feldspar with rising temperature.

*Orthopyroxene*

Opx is present in the experiments at temperatures above 925°C at 7 kbar, and at 1050 and 1035°C in both starting materials at 10 and 12·5 kbar, respectively. It is also present in the run product of 1000°C PON experiment at 15 kbar. In these experimental run products, opx has a characteristic prismatic to acicular habit, and clots of opx crystals commonly pseudomorph biotite (Fig. 3). The opx grains have high $Al_2O_3$ (6·8–7·9 wt % and 5·1–9·8 wt % in PON and KAL, respectively), consistent with their high temperatures of formation. The $Al_2O_3$ content of opx increases with rising temperature at constant pressure. Opx also has a lower Mg-number than coexisting biotite.

*Fe–Ti oxides*

Ilmenite is the dominant Fe–Ti oxide mineral in most of the run products. At pressures ≥10 kbar, it is accompanied by rutile. The hematite component of ilmenite is low and varies from ~3 to 7 mol % in both KAL and PON. Rutile grains were not analyzed quantitatively.

*Melt*

Glass (quenched melt) is present in all the run products, and increases in abundance with rising temperature. It occurs mostly as thin films around biotite and garnet and also as isolated pockets. Although the melt pockets were too small to obtain reliable analyses in most cases, the available data indicate that the melts are peraluminous and remain leucocratic to high temperatures.

## DISCUSSION

### Approach to equilibrium

We suggest a close approach to equilibrium in our experiments on the basis of three lines of evidence. The most rigorous evidence is provided by successful phase reversals. The first appearance of opx was reversed at 7 and 10 kbar in both starting materials (see Fig. 3 and Table 2). Second, most of the phases in the run products

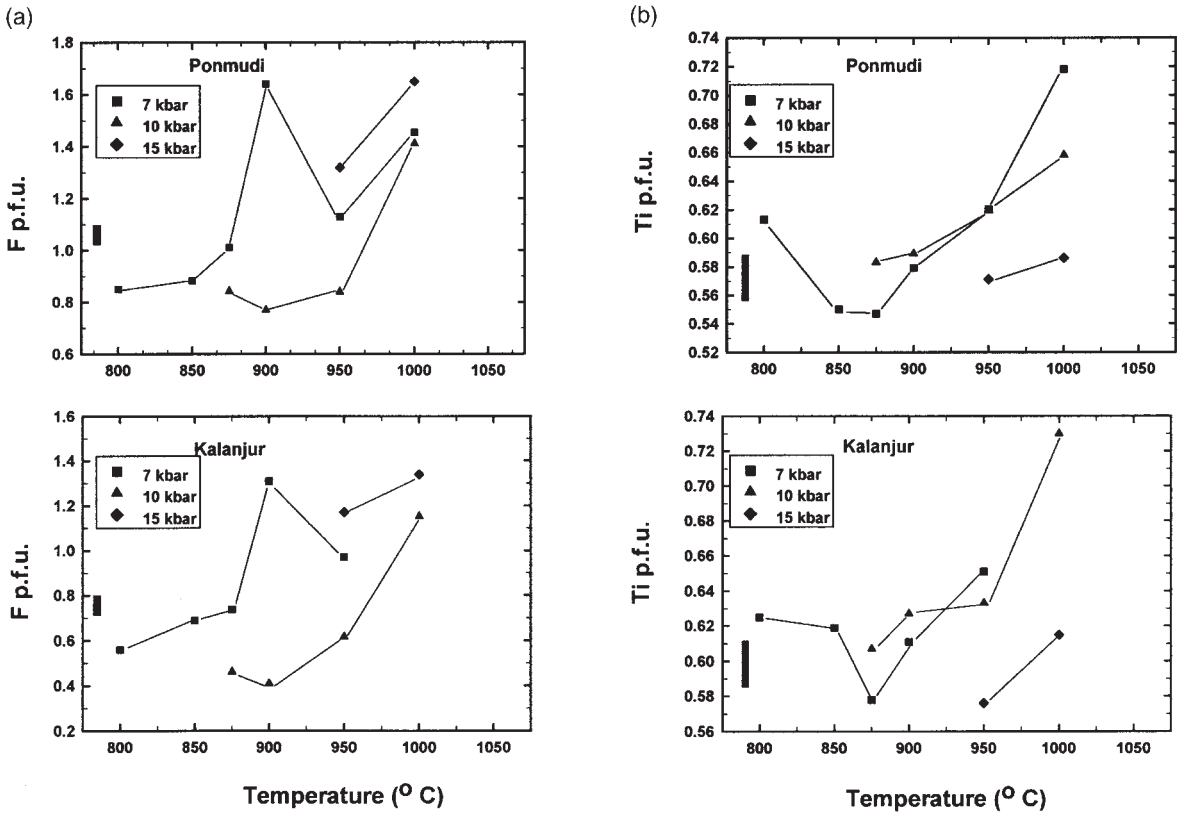


**Fig. 5.** Biotite compositions. (a) F (per formula unit). vs temperature. (b) Ti (per formula unit) vs temperature. Bars represent 1σ standard deviation.

were compositionally homogeneous, suggesting an approach to equilibrium. Garnet was the only phase that showed significant heterogeneity in composition within a single run product. The larger garnet crystals were compositionally similar to the starting garnet whereas the smaller euhedral garnets were closer to being in equilibrium at experimental *P–T* conditions. Compositional equilibration in garnet was also found to be a problem in many previous fluid-absent melting experiments (e.g. Le Breton & Thompson, 1988; Carrington & Harley, 1995). Nevertheless, changes in garnet composition in the higher temperature and/or pressure experiments suggest that the phase was at least reactive during the experiments. Third, the abundance of phases changed in a consistent manner with temperature and pressure. Most notable among these changes was the decrease in the abundance of biotite and plagioclase with rising temperature, the increase in abundance of garnet with rising temperature and pressure, and the appearance and increase in abundance of opx with rising temperature in the 7 kbar experiments. Phases generally also showed consistent variation in composition with temperature and pressure, with the clearest compositional trends noted in plagioclase, alkali feldspar and biotite. With the exception of garnet, all the phases present in the run products had a different composition from that of the starting material.

## Melting reactions

### *Fluid-present melting*

Trace amounts of melt (<5%) were identified in experiments at temperatures below 875–900°C. However, at these lower temperatures no significant compositional variation was observed in biotite or other Fe–Mg-bearing phases, which suggests limited participation of these phases in the melting process. We interpret the quenched melt observed at these low temperatures to be the result of fluid-present melting. Despite the extreme care taken to eliminate moisture during sample preparation and loading, the hygroscopic nature of the finely powdered starting materials invariably results in the adsorption of some $H_2O$. At experimental temperatures, which in this study exceeded the $H_2O$-saturated solidus by 150°C or more, the presence of even small amounts of moisture (0·5 wt %) would result in non-negligible amounts of vapor-saturated melting. The small amount of adsorbed

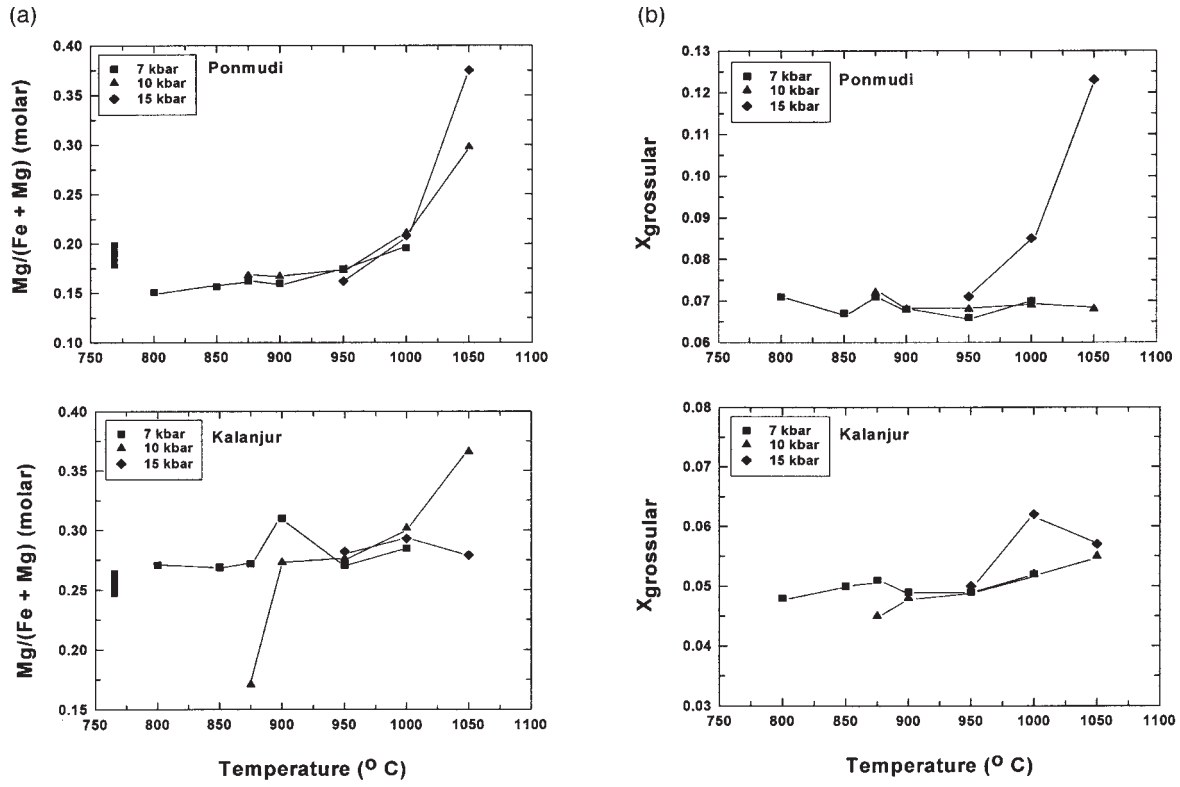


**Fig. 6.** Garnet compositions. (a) Molar Mg/(Fe + Mg) vs temperature. (b) $X_{grossular}$ vs temperature. Bars represent 1σ standard deviation.

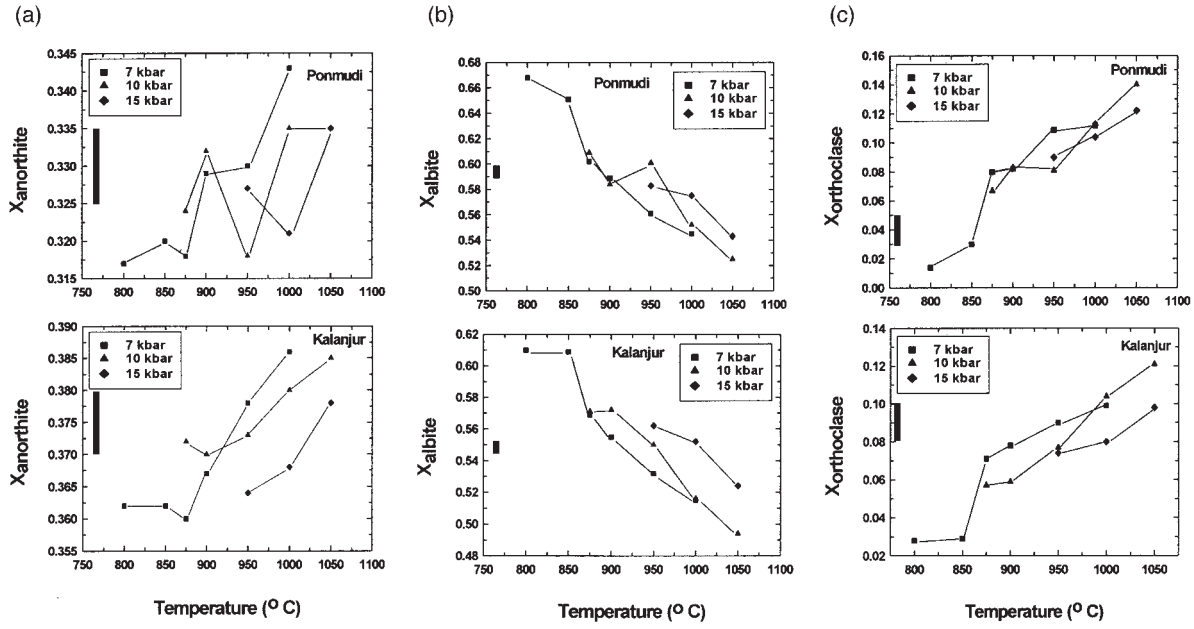


**Fig. 7.** Plagioclase compositions. (a) $X_{anorthite}$ vs temperature. (b) $X_{albite}$ vs temperature. (c) $X_{orthoclase}$ vs temperature. Bars represent 1σ standard deviation.

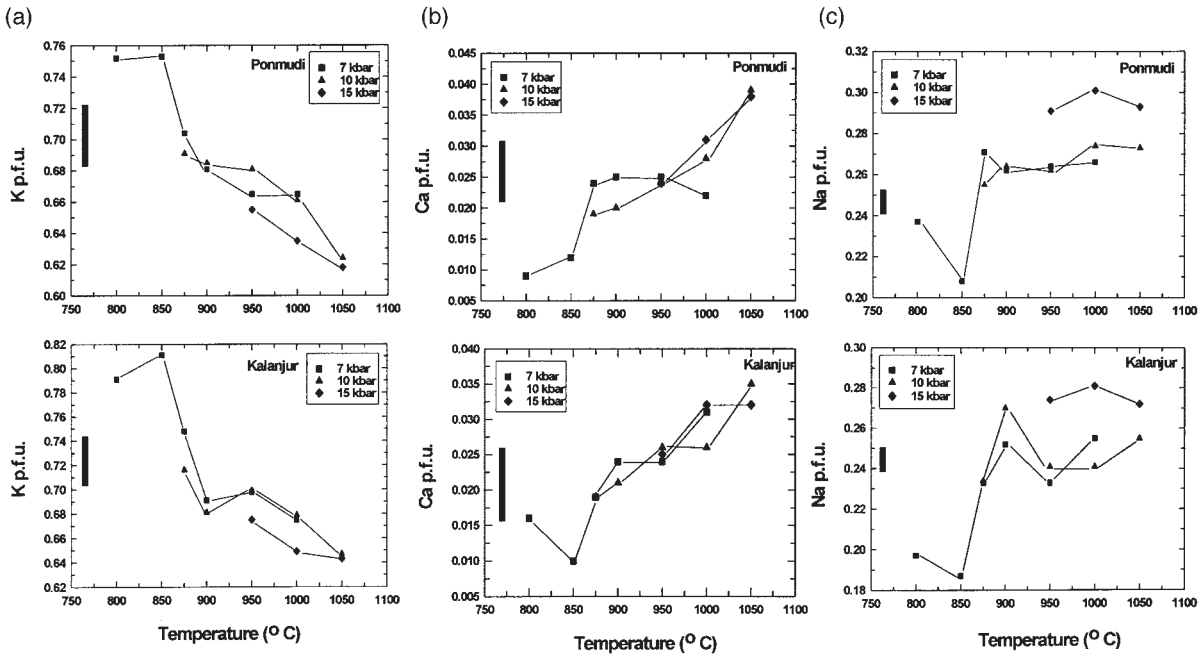


**Fig. 8.** Alkali feldspar compositions. (a) K (per formula unit) vs temperature. (b) Ca (per formula unit) vs temperature. (c) Na (per formula unit) vs temperature. Bars represent 1σ standard deviation.

water would rapidly dissolve in this melt, leading to the establishment of fluid-absent conditions.

### *Fluid-absent solidus*

Melt production accompanied by significant changes in the modal abundance and composition of biotite was taken as the criterion for the onset of fluid-absent melting. Accordingly, 875°C is taken as the fluid-absent solidus for PON and KAL at 7 kbar. At 10 kbar, phase compositional variations are generally more pronounced above 900°C, which is therefore inferred to be the position of fluid-absent solidus at this pressure.

The phase relations are consistent with a fluid-absent solidus reaction of the type

$$\text{Biotite} + \text{Plagioclase} + \text{Quartz} = \text{Garnet} + \text{K-feldspar} + \text{Melt}. \quad (1)$$

This is interpreted from an increase in modal abundance of garnet and alkali feldspar concomitant with a decrease in biotite and plagioclase proportions in experiments at temperatures exceeding the fluid-absent solidus.

### *Orthopyroxene-in reaction*

The second reaction, which was the principal focus of the present study, corresponds to the first appearance of opx (Fig. 9). On the basis of the decrease of biotite and plagioclase concomitant with the appearance and increase of opx and garnet with rising temperature, we interpret the opx-forming reaction to be

$$\text{Biotite} + \text{Plagioclase} + \text{Quartz} = \text{Orthopyroxene} + \text{Garnet} + \text{K-feldspar} + \text{Melt}. \quad (2)$$

Progress of reactions (1) and (2) leaves a residual biotite higher in Ti, F and Mg and lower in Al (see discussion on biotite composition above).

Reaction (2) has a relatively shallow positive slope between 7 and 10 kbar but steepens above 10 kbar and may in fact bend back at higher pressure to a negative $dP/dT$ slope. The back-bending of reaction (2) was documented in PON, in which opx was observed in the run product at 1035 and 1000°C at 12·5 and 15 kbar, respectively. In KAL, however, opx was not observed at 15 kbar. Nevertheless, the occurrence of opx in the 1035°C, 12·5 kbar experiment confirms a steepening of the reaction curve.

We attribute the steepening in the slope of the opx-in curve at high pressures to a significant change in the reaction stoichiometry, such that the volume change of the reaction changes from positive to negative. This is evident from changes in the modal abundance of reactant and product minerals with increasing pressure without significant changes in the proportion of melt produced. With increasing pressure (at constant $T$), changes include increase in the modal abundance of biotite, garnet and alkali feldspar, and a decrease in the abundance of plagioclase and opx. The

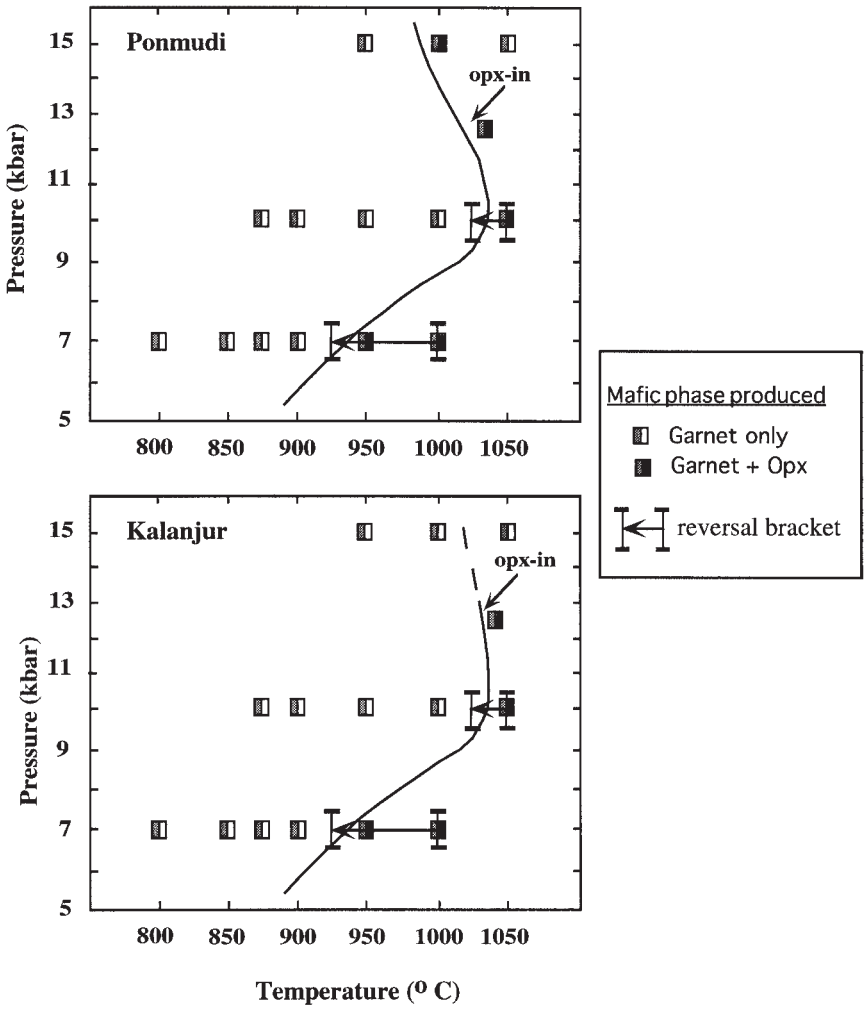


**Fig. 9.** *P–T* location of the orthopyroxene-in curve obtained in the present study.

residual plagioclase in the high-pressure experiments is also markedly more albite rich than in the low-pressure experiments. These observations suggest increased production of garnet through the melting reaction at the expense of plagioclase and opx. Biotite contributes proportionately less (relative to plagioclase) to the melting reaction at high pressure (see Patiño Douce & Beard, 1995).

## Comparison of melting reactions with previous studies

The results of this study provide interesting comparisons with the studies of Vielzeuf & Montel (1994), Patiño Douce & Beard (1995, 1996) and Stevens *et al.* (1997), who also investigated the fluid-absent melting behavior of similar semi-pelitic bulk compositions (Table 3). In particular, the starting materials of all the experimental studies contained biotite, plagioclase and quartz, the necessary reactants for fluid-absent melting reactions (1) and (2) to occur. There were, however, also some differences in our experimental starting materials, such as the presence of K-feldspar and a significantly lower modal proportion of biotite. As discussed above, the most important difference was the composition of biotite.

### *Fluid-absent solidus*

The fluid-absent solidus reaction (1) inferred in our study is consistent with the observation of Vielzeuf & Montel (1994) that, at pressures >5 kbar, the beginning of melting does not coincide with the formation of opx but is

*Table 3: Bulk-rock and mineral composition of starting materials used in previous fluid-absent melting studies compared with that of the present study*

| Study: | V&M (1994) | P&B (1995) | P&B (1996) | St *et al.* (1997) | St *et al.* (1997) | This study* | This study* |
|---|---|---|---|---|---|---|---|
| Sample: | CEVP | SBG | SMAG | A | NB | Ponmudi | Kalanjur |
| $SiO_2$ | 69·99 | 63·60 | 62·30 | 66·37 | 66·33 | 68·80 | 68·00 |
| $TiO_2$ | 0·70 | 2·50 | 2·80 | 0·00 | 0·87 | 0·83 | 0·94 |
| $Al_2O_3$ | 12·96 | 12·30 | 11·90 | 12·62 | 14·34 | 14·60 | 14·40 |
| $FeO^T$ | 4·87 | 7·60 | 11·70 | 8·81 | 6·53 | 5·99 | 6·22 |
| MnO | 0·06 | 0·10 | 0·20 | 0·01 | 0·01 | 0·08 | 0·11 |
| MgO | 2·36 | 4·60 | 1·84 | 4·75 | 3·45 | 1·05 | 1·56 |
| CaO | 1·67 | 2·10 | 2·10 | 1·26 | 0·91 | 2·13 | 2·45 |
| $Na_2O$ | 2·95 | 1·90 | 2·00 | 1·31 | 0·95 | 2·55 | 2·40 |
| $K_2O$ | 2·41 | 3·60 | 3·40 | 3·58 | 2·59 | 4·42 | 3·63 |
| Whole-rock $X_{Mg}$ | 47 | 52 | 22 | 49 | 58 | 23 | 31 |
| wt % Ti in biotite | 2·8 | 3·9 | 4·6 | 0 | 2·3 | 5·0 | 5·4 |
| wt % F in biotite | n | 0·3 | 0·1 | n | n | 1·3 | 1·4 |
| $X_{Mg}$ in biotite | 0·44 | 0·55 | 0·23 | 0·49 | 0·58 | 0·46 | 0·56 |
| $X_{An}$ in plagioclase | 22 | 38 | 38 | 35 | 35 | 32 | 37 |
| wt % $Al_2O_3$ in biotite | 19·5 | 14·4 | 13·2 | 16·2 | 20·2 | 13·7 | 13·6 |
| Modal % biotite | 25 | 37·2 | 37·2 | 39 | 39 | 10 | 11 |

V&M (1994), Vielzeuf & Montel (1994); P&B (1995), Patiño Douce & Beard (1995); P&B (1996), Patiño Douce & Beard (1996); St *et al.* (1997), Stevens *et al.* (1997). $X_{Mg}$, molar Mg/(Fe + Mg); n, not given; $X_{An}$, molar Ca/(Ca + Na + K).
*Chacko (1987).

associated instead with a garnet-producing reaction. In contrast to the present results, however, Vielzeuf & Montel (1994) did not find alkali feldspar in their experimental products and interpreted the increase in the orthoclase component of the plagioclase to indicate that alkali feldspar was a product phase. The phase relations reported by Patiño Douce & Beard (1996) at pressures >10 kbar are also consistent with solidus reaction (1), although they too did not report alkali feldspar in their run products. In the more magnesian bulk compositions studied by Patiño Douce & Beard (1995) and Stevens *et al.* (1997), the fluid-absent solidus coincided with an opx-forming reaction. These differences in phase relations probably reflect the strong control of Fe–Mg ratio on the stability of opx relative to garnet (see Patiño Douce & Beard, 1996).

All of the studies noted above found a steep $dP/dT$ slope for the solidus reaction. This is corroborated by the present study, where fluid-absent melting was inferred to begin at 875°C at 7 kbar and between 875 and 900°C at 10 kbar. The major difference in the results of the present study is that the temperature of the fluid-absent solidus is up to 90°C higher than reported in earlier studies. We attribute this difference to the higher Ti and F content of biotite in the starting materials used in the present experiments. This interpretation is consistent with the observations made in synthetic systems that the presence of these elements extends the stability of biotite to higher temperatures under fluid-absent conditions (Forbes & Flower, 1974; Trønnes *et al.*, 1985; Peterson *et al.*, 1991; Dooley & Patiño Douce, 1996). In contrast to this interpretation, Stevens *et al.* (1997) argued that Ti substitution in biotite does not affect the temperature of the fluid-absent solidus, although it does extend the temperature range over which biotite undergoes fluid-absent melting. They based this conclusion on the similarity of solidus temperatures obtained with their Ti-bearing and Ti-free starting materials (Table 3). However, comparison of the solidus temperatures reported by Stevens *et al.* (1997) (~800–835°C) with those of Patiño Douce & Beard (1995) (850–875°C) and the present study (875–900°C) suggests that increasing the Ti content of biotites with comparable Mg-number significantly raises the solidus temperature. The apparent absence of a stabilizing effect of Ti in the Stevens *et al.* (1997) experiments may be due to the fact that their high-Ti biotite ('NB') was also ~20% higher in Al than their Ti-free biotite ('A'). As noted above, compositional

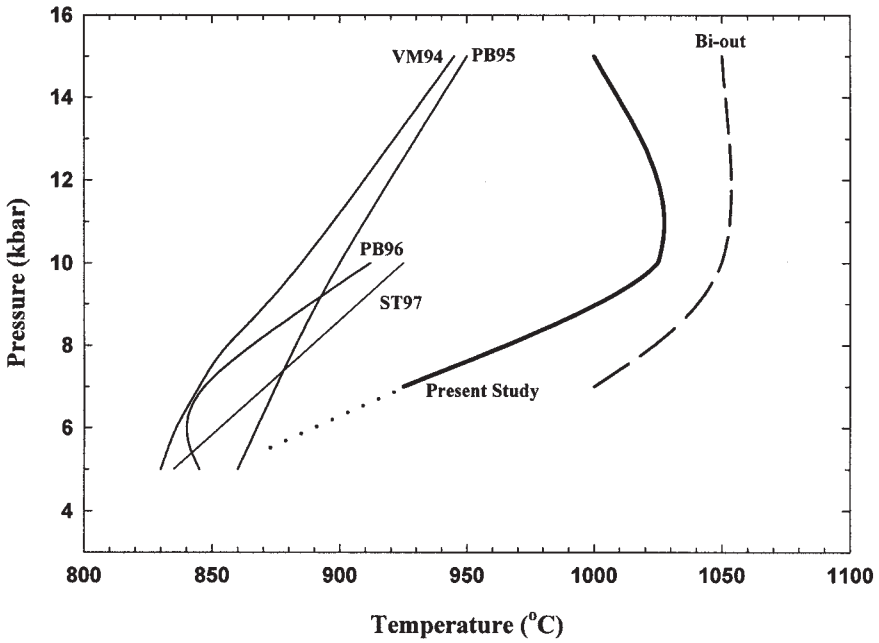


**Fig. 10.** *P–T* diagram comparing the orthopyroxene-in curve obtained in this study with those from previous fluid-absent melting studies. ST97, Stevens *et al.* (1997); PB96, Patiño Douce & Beard (1996); PB95, Patiño Douce & Beard (1995); VM94, Vielzeuf & Montel (1994).

trends in the biotites of the present experiments suggest that Al-rich biotite breaks down at lower temperature than Al-poor biotite. Thus, in the Stevens *et al.* experiments, the stabilizing effect of Ti in biotite may have been masked by the destabilizing effect of high Al.

### *Orthopyroxene-in reaction*

Figure 10 compares the *P–T* location of the opx-in reaction (biotite + plagioclase + quartz = orthopyroxene ± garnet ± K-feldspar + melt) determined in the present study with those from four earlier experimental studies on semi-pelitic bulk compositions. Our experiments indicate that significantly higher temperatures are required for opx formation by fluid-absent melting (>50°C higher at 7 kbar, and >100°C higher at 10 kbar). We again attribute this result to the higher Ti and F content of the starting biotites of our study relative to those of earlier studies. It could be argued that even if biotites of the previous experimental studies had lower initial Ti and F, the concentrations of these elements should have increased during the experiments to reflect the equilibrium compositions at the new, higher-temperature conditions. If this process occurs at the early stages of experiments, biotite compositions in all experimental studies would be similar at the onset of fluid-absent melting, and should therefore yield comparable temperatures for opx formation. We suggest two reasons why this early-stage adjustment of biotite compositions did not occur in previous experiments. First, two of the earlier studies (Vielzeuf & Montel, 1994; Stevens *et al.*, 1997) did not report a Ti-saturating phase (e.g. ilmenite) in their starting material, and none of the earlier experiments reported an F-saturating phase. In such cases, the only way to increase the Ti or F content of the biotite under fluid-absent conditions is through progress of melting reactions (1) and (2). This in turn allows for garnet and/or opx formation at lower temperature than is possible in experiments with high-Ti and -F starting biotites. Second, even in cases where a small amount of a Ti-saturating phase is present in the starting material (Patiño Douce & Beard, 1995, 1996), the establishment of Ti-exchange equilibrium between this phase and biotite is inhibited by the relatively low diffusivities of elements in granitic melts (Baker, 1991). Thus, some biotite grains may undergo fluid-absent melting to form anhydrous phases before Ti-exchange equilibrium with ilmenite is achieved. The simplest way to avoid these potential kinetic problems is to use a biotite starting material that closely approximates compositions found in rocks on the verge of the granulite facies. We argue that our biotite starting materials more faithfully reflect such compositions and, therefore, that the *P–T* position of the opx-in reaction obtained in our study is a more realistic representation of fluid-absent opx formation in natural semi-pelites.

The present study indicates a positive slope for the opx-in reaction between 7 and 10 kbar, consistent with previous studies. However, the reaction between 7 and

10 kbar has a much shallower d$P$/d$T$ slope (~33°C/kbar) than found in other studies [~10°C/kbar, Vielzeuf & Montel (1994); ~8°C/kbar, Patiño Douce & Beard (1995); ~25°C/kbar, Patiño Douce & Beard (SMAG, 1996)]. This could also be attributed to the dependence of the stoichiometry of reaction (2) on the bulk composition of the starting materials (e.g. a higher alumina content of biotite may favor the reaction at slightly lower temperatures at higher pressures). None of the previous studies documented a reversal in the slope of the opx-in reaction between 10 and 15 kbar.

*Biotite fluid-absent melting interval*

The $P$–$T$ span over which biotite fluid-absent melting occurs in the present study is represented by the combination of multivariant fields of the solidus reaction (1) and the opx-in reaction (2). The position of the biotite-out curve in Fig. 10 is an estimated minimum, as it was not tightly bracketed in the experiments. Fluid-absent melting involving biotite is completed over a temperature interval of 125–200°C during which the melt fraction increases gradually. This range is broadly consistent with the melting interval observed in other studies, except at 10 kbar where biotite persists in the run products for temperatures 50–75°C above those of previous studies (see Vielzeuf & Montel, 1994; Patiño Douce & Beard, 1995, 1996; Stevens *et al.*, 1997). The temperature interval over which biotite, garnet and melt coexist without opx increases with pressure up to 10 kbar and then decreases; because of the slope reversal of the opx-in reaction between 10 and 15 kbar, the width of this multivariant field decreases. The interval over which biotite, opx, garnet and melt coexist is about 25–75°C, which is conformable with the intervals reported by Vielzeuf & Montel (1994) and Patiño Douce & Beard (1995, 1996).

*Effect of Mg-number on opx formation*

The biotite in the two starting materials of the present experiments differed in Mg-number by about 10 units (0·46 for PON; 0·56 for KAL). Within the temperature resolution of the experiments, there was no marked difference in the melting behavior, which suggests that moderate differences in the Mg-number of biotite do not greatly affect phase relations during fluid-absent melting. Nevertheless, the partitioning of Mg into biotite relative to coexisting opx or garnet suggests that, in general, the initial temperature of opx formation should rise with increasing Mg-number of the starting biotite. This effect is mitigated somewhat by the influence of bulk-rock Mg-number on the stability fields of garnet and opx. Decreasing bulk-rock Mg-number favors the formation of garnet as the primary ferromagnesian phase associated with fluid-absent melting of biotite-bearing, peraluminous rocks, and restricts opx stability to higher temperatures. The net result of these two competing factors is a relatively small influence of Mg-number on the temperature required for the first appearance of opx (see Patiño Douce & Beard, 1996; Stevens *et al.*, 1997).

## Granulite formation at Ponmudi and Kalanjur

The most direct application of the results of this study is in evaluating the petrogenesis of granulites at Ponmudi and Kalanjur, the two localities from which the starting materials were obtained. Many workers have interpreted the field relationships at incipient granulite localities such as these to reflect a fluid-present dehydration process, in which the breakdown of biotite or hornblende was triggered by the local influx of low water activity fluids (e.g. Janardhan *et al.*, 1979; Ravindra Kumar *et al.*, 1985; Ravindra Kumar & Chacko, 1986). Others, however, have argued that these or broadly similar features were the result of fluid-absent partial melting (Waters, 1988; Burton & O'Nions, 1990). The $P$–$T$ position of the opx-in curve determined in the present study provides insight on the nature of the granulite-forming process at these localities.

Metamorphic $P$–$T$ conditions determined for the granulites at Ponmudi and Kalanjur are 780°C, 5·2 kbar and 760°C, 5·9 kbar, respectively (Chacko *et al.*, 1996). By comparison, extrapolation of the present experimental results to 5–6 kbar indicates that a temperature of at least 875°C is required to stabilize opx by fluid-absent melting. Thus, temperature estimates for the Ponmudi and Kalanjur rocks are too low to be consistent with granulite formation by a fluid-absent melting process. One might argue that peak metamorphic temperature at these localities was in fact much higher than ~780°C, but that the mineral equilibria used in calculating temperature significantly re-equilibrated during slow cooling of the rocks. However, the temperature estimates for the two localities are based on aluminum solubility in opx (the refractory garnet–Al-in-opx thermobarometer), and are therefore likely to be a faithful representation of peak metamorphic temperature. Qualitatively, this can be corroborated by comparing the relatively low $Al_2O_3$ content (3·2–3·5 wt %) of opx from the Ponmudi and Kalanjur granulites (Srikantappa *et al.*, 1985; Chacko *et al.*, 1987) with that of the opx formed at high temperature in the present experiments (5–9·8 wt % $Al_2O_3$).

Another way of representing the discrepancy between our fluid-absent experimental results and the granulite-forming process at Ponmudi and Kalanjur is to compare water activities associated with the first appearance of opx. For rocks or experimental charges containing biotite, quartz, opx and alkali feldspar, $a(H_2O)$ can be calculated with the equilibrium $2KMg_3AlSi_3O_{10}(OH)_2 + 6SiO_2 =$

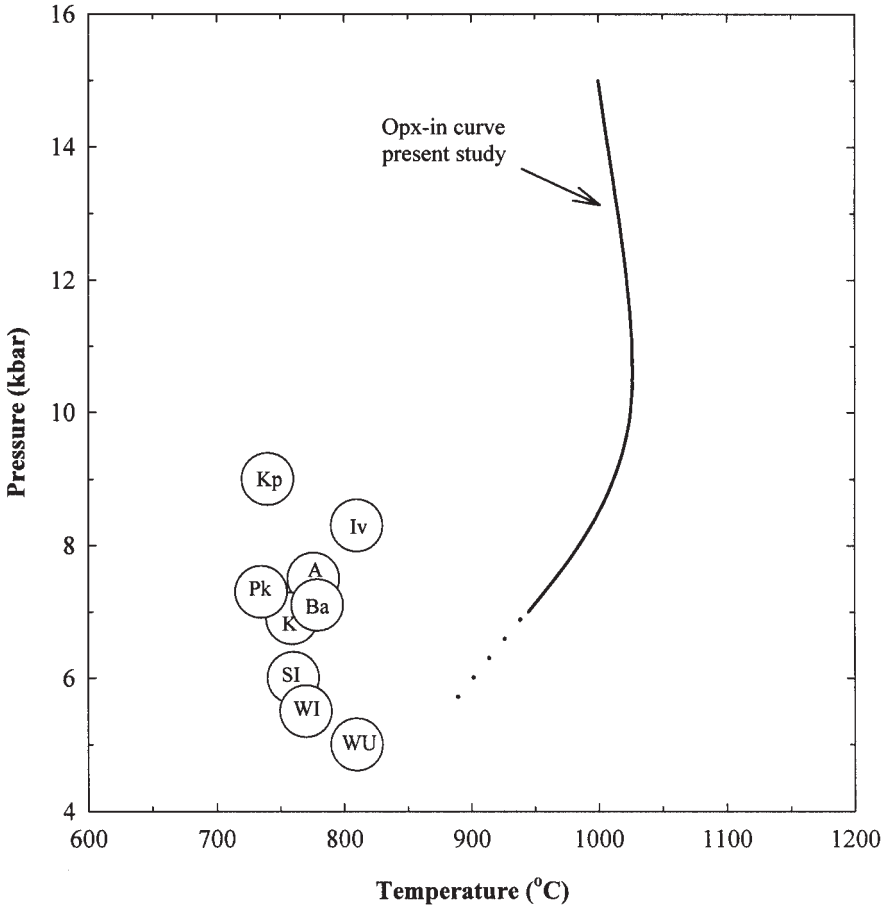


**Fig. 11.** Comparison of reported peak metamorphic *P–T* conditions of transitional amphibolite–granulite terranes with the *P–T* conditions required for orthopyroxene formation under fluid-absent conditions. Transitional terrane data: SI (South India and Sri Lanka), Janardhan *et al.* (1982) and Hansen *et al.* (1987), respectively; Iv (Ivrea Zone), Henk *et al.* (1997); Pk (Pikwitonei), Paktunc & Baer (1986); A (Adirondacks), Bohlen *et al.* (1985); Kp (Kapuskasing), Percival (1983); K (Kurenegala, Sri Lanka), Burton & O'Nions (1990); WU (West Ussimaa), Schreurs (1985); Ba (Bamble), Lamb *et al.* (1986); Wi (Willyama Complex), Phillips & Wall (1981).

$2KAlSi_3O_8 + 3Mg_2Si_2O_6 + 2H_2O$. We used the thermodynamic data of Holland & Powell (1998) in our calculations and assumed ideal on-site mixing in biotite, opx and alkali feldspar. $a(H_2O)$ values for the 950°C, 7 kbar PON and KAL experiments are 0·88 and 0·61, respectively. These $a(H_2O)$ values, which reflect internal buffering in the experimental charges by fluid-absent melting reactions, are much higher than values calculated for incipient granulites from the Ponmudi (0·27) and Kalanjur (0·31) localities at the inferred metamorphic *P–T* conditions. This indicates that water activities must be considerably lower than those to which the experiments were internally buffered before opx will be stabilized in these rocks at $T$ <800°C. One way to generate the requisite low water activities is through the influx of $CO_2$-rich ( Janardhan *et al.*, 1979) or hypersaline (Newton *et al.*, 1998) fluids. As has been demonstrated experimentally in the Mg-end-member system ($MgO–KAlO_2–SiO_2–H_2O \pm CO_2 \pm KCl$), such fluids can destabilize phlogopite and induce opx growth at significantly lower temperatures than is possible under fluid-absent conditions (Peterson & Newton, 1989; Clemens *et al.*, 1997; Aranovich & Newton, 1998). For example, an NaCl–KCl brine ($XH_2O = 0·4$) lowers $a(H_2O)$ below 0·3 at 5–6 kbar and 760°C (Newton *et al.*, 1998), which is low enough to induce opx growth in these rocks at $T$ <800°C. This fluid-present mechanism of granulite formation can be evaluated further by experimentally determining the temperatures required for opx formation with the PON and KAL starting materials in the presence of carbonic or saline fluids.

### Implications for the orthopyroxene isograd and deep crustal processes

If, as argued in this paper, the starting materials of our experiments are representative of rocks found near the amphibolite- to granulite-facies transition, then the present results have important implications for the interpretation of regional opx-in isograds. Figure 11 compares *P–T* constraints for fluid-absent opx formation derived in this study with those reported for a number of transitional amphibolite–granulite terranes worldwide. In all of these terranes, opx has been noted in rocks with bulk composition broadly similar to those investigated in the present study. Our results indicate that the temperatures reported for these transitional terranes are at least 75–100°C too low to allow for opx formation by fluid-absent melting. These temperatures are also inconsistent with the opx-in curves of previous experimental studies, albeit with a smaller temperature discrepancy.

One explanation for the large temperature discrepancy is that temperatures reported for these transitional terranes do not represent peak metamorphic temperatures. Most of the temperature estimates for the terranes shown in Fig. 11 were derived from Fe–Mg exchange geothermometry, and retrograde resetting of such thermometers is known to be a common problem in high-grade, slowly cooled rocks (e.g. Frost & Chacko, 1989; Spear & Florence, 1992). Thus, it is possible that peak temperatures in these terranes were actually much higher than indicated by the exchange geothermometers, and comparable with those required to form opx by fluid-absent melting. This implies, however, that temperatures of crustal metamorphism commonly exceed 850–900°C. By comparison, existing thermal models of collisional orogenic belts suggest that temperatures in excess of 900°C are not generally achieved, even at the base of crust that has been tectonically thickened to 55–70 km (England & Thompson, 1986; Patiño Douce *et al.*, 1990; Ashwal *et al.*, 1992). Therefore, rationalization of these high temperatures requires either significant adjustment of some of the input parameters in these thermal models (e.g. values for crustal radioactive heat production) or the presence in transitional terranes of secondary heat sources such as mafic or charnockitic magmas. On the other hand, if a 700–800°C temperature estimate for a particular transitional terrane truly represents a peak metamorphic temperature, then our results imply that opx in that terrane formed by a process other than fluid-absent melting. The relative merits of these alternative proposals must be evaluated on a case-by-case basis. Nevertheless, we suggest that the widely held notion that granulite-facies mineral assemblages develop at 700–800°C by fluid-absent processes be abandoned as it is inconsistent with the results of both the present and earlier experimental studies. Either peak metamorphic temperatures in transitional amphibolite–granulite terranes were significantly higher than reported or the granulite-forming process was not fluid absent.

## ACKNOWLEDGEMENTS

We thank Bob Luth for advice and support in the experimental petrology laboratory at the University of Alberta, Dave Pattison for advice on manuscript revisions, and Lang Shi for assistance with the electron probe microanalysis. We also thank Alberto Patiño Douce, Bruno Scaillet and particularly Ron Frost for constructive reviews. This work was supported by an NSERC research grant to T.C.

## REFERENCES

Andersen, D. J., Lindsley, D. H. & Davidson, P. M. (1993). QUIlF: a Pascal program to assess equilibria among Fe–Mg–Mn–Ti oxides, pyroxenes, olivine and quartz. *Computers and Geosciences* **19**, 1333–1350.

Aranovich, L. Y. & Newton, R. C. (1998). Reversed determination of the reaction: phlogopite + quartz = enstatite + potassium feldspar + $H_2O$ in the ranges 750–875°C and 2–12 kbar at low $H_2O$ activity with concentrated KCl solutions. *American Mineralogist* **83**, 193–204.

Ashwal, L. D., Morgan, P. & Hoisch, T. D. (1992). Tectonics and heat sources for granulite metamorphism of supracrustal-bearing terranes. *Precambrian Research* **55**, 525–538.

Baker, D. R. (1991). Interdiffusion of hydrous dacitic and rhyolitic melts and the efficacy of rhyolite contamination by dacitic enclaves. *Contribution to Mineralogy and Petrology* **106**, 462–473.

Berman, R. G. (1988). Internally consistent thermodynamic data for stoichiometric minerals in the system $Na_2O$–$K_2O$–$Fe_2O_3$–$Al_2O_3$–$SiO_2$–$TiO_2$–$H_2O$–$CO_2$. *Journal of Petrology* **29**, 445–522.

Bohlen, S. R., Valley, J. W. & Essene, E. J. (1985). Metamorphism in the Adirondacks: I, Petrology, pressure and temperature. *Journal of Petrology* **26**, 971–992.

Burton, K. W. & O'Nions, R. K. (1990). The timescale and mechanism of granulite formation at Kurunegala, Sri Lanka. *Contributions to Mineralogy and Petrology* **106**, 66–89.

Carrington, D. P. & Harley, S. L. (1995). Partial melting and phase relations in high-grade metapelites: an experimental petrogenetic grid in the KFMASH system. *Contributions to Mineralogy and Petrology* **120**, 270–291.

Carrington, D. P. & Watt, G. R. (1995). A geochemical and experimental study of the role of K-feldspar during water-undersaturated melting of metapelites. *Chemical Geology* **132**, 59–76.

Chacko, T. (1987). Petrologic, geochemical and isotopic studies in the charnockite–khondalite terrain of southern Kerala, India: the deposition and granulite-facies metamorphism of a Precambrian sedimentary sequence. Ph.D. thesis, University of North Carolina at Chapel Hill, 191 pp.

Chacko, T., Ravindra Kumar, G. R. & Newton, R. C. (1987). Metamorphic conditions in the Kerala (south India) Khondalite Belt: a granulite-facies supracrustal terrain. *Journal of Geology* **96**, 343–358.

Chacko, T., Ravindra Kumar, G. R., Meen, J. K. & Rogers, J. J. W. (1992). Geochemistry of high-grade supracrustal rocks from the Kerala Khondalite Belt and adjacent massif charnockites, South India. *Precambrian Research* **55**, 469–489.

Chacko, T., Lamb, M. & Farquhar, J. (1996). Ultra-high temperature metamorphism in the Kerala Khondalite Belt. In: Santosh, M. & Yoshida, M. (eds) *The Archean and Proterozoic Terrains in Southern India and East Gondwana. Gondwana Research Group Memoir* **3**, 157–165.

Clemens, J. D. (1992). Partial melting and granulite genesis: a partisan overview. *Precambrian Research* **55**, 297–301.

Clemens, J. D., Droop, G. T. R. & Stevens, G. (1997). High-grade metamorphism, dehydration and crustal melting: a reinvestigation based on new experiments in the silica-saturated portion of the system $KAlO_2$–MgO–$SiO_2$–$H_2O$–$CO_2$ at $P \leq 1{\cdot}5$ GPa. *Contributions to Mineralogy and Petrology* **129**, 308–325.

Dooley, D. F. & Patiño Douce, A. E. (1996). Fluid-absent melting of F-rich phlogopite + rutile + quartz. *American Mineralogist* **81**, 202–212.

Eckert, J. O., Hatcher, R. D. & Mohr, D. W. (1989). The Wayah granulite-facies metamorphic core, southwestern North Carolina: high-grade culmination of Taconic metamorphism in the southern Blue Ridge. *Geological Society of America Bulletin* **101**, 1434–1447.

Elkins, L. T. & Grove, T. L. (1990). Ternary feldspar experiments and thermodynamic models. *American Mineralogist* **75**, 544–559.

Elvevold, S., Scrimgeour, I., Powell, R., Stuwe, K. & Wilson, J. L. (1994). Reworking of deep-seated gabbros and associated contact metamorphosed paragneisses in the south-eastern part of the Seiland Igneous Province, northern Norway. *Journal of Metamorphic Geology* **12**, 539–556.

England, P. C. & Thompson, A. B. (1986). Some thermal and tectonic models for crustal melting in continental collision zones. In: Coward, M. P. & Ries, A. C. (eds) *Collision Tectonics. Geological Society, London, Special Publications* **19**, 83–94.

Forbes, W. C. & Flower, M. F. J. (1974). Phase relations of titan-phlogopite, $K_2Mg_4TiAl_2Si_6O_{20}(OH)_4$: a refractory phase in the upper mantle? *Earth and Planetary Science Letters* **22**, 60–66.

Franz, L. & Harlov, D. E. (1998). High-grade K-feldspar veining in granulites from the Ivrea–Verbano Zone, Northern Italy: fluid flow in the lower crust and implications for granulite facies genesis. *Journal of Geology* **106**, 455–472.

Frost, B. R. & Chacko, T. (1989). The granulite uncertainty principle: limitations on thermobarometry in granulites. *Journal of Geology* **97**, 435–450.

Fyfe, W. S. (1973). The granulite facies, partial melting and the Archean crust. *Philosophical Transactions of the Royal Society of London* **273**, 457–461.

Ghiorso, M. S. (1990). Thermodynamic properties of hematite–ilmenite–geikielite solid solutions. *Contributions to Mineralogy and Petrology* **104**, 645–667.

Grant, J. A. & Frost, B. R. (1990). Contact metamorphism and partial melting of pelitic rocks in the aureole of the Laramie Anorthosite Complex, Morton Pass, Wyoming. *American Journal of Science* **290**, 425–472.

Hansen, E. C., Janardhan, A. S., Newton, R. C., Prame, W. K. B. N. & Ravindra Kumar, G. R. (1987). Arrested charnockite formation in southern India and Sri Lanka. *Contributions to Mineralogy and Petrology* **96**, 225–244.

Henk, A., Franz, L., Teufel, S. & Oncken, O. (1997). Magmatic underplating, extension and crustal reequilibration—insights from a cross section through the Ivrea Zone and Strona–Ceneri Zone, northern Italy. *Journal of Geology* **105**, 367–377.

Holland, T. & Powell, R. (1998). An internally consistent thermodynamic data set for phases of petrological interest. *Journal of Metamorphic Geology* **16**, 309–343.

Janardhan, A. S., Newton, R. C. & Smith, J. V. (1979). Ancient crustal metamorphism at low $P_{H_2O}$: charnockite formation at Kabbaldurga, south India. *Nature* **278**, 511–514.

Janardhan, A. S., Newton, R. C. & Hansen, E. C. (1982). The transformation of amphibolite facies gneiss to charnockite in southern Karnataka and northern Tamil Nadu, India. *Contributions to Mineralogy and Petrology* **79**, 130–149.

Kushiro, I. (1976). A new furnace assembly with a small temperature gradient in solid-media, high pressure apparatus. *Carnegie Institution of Washington Yearbook* **68**, 231–233.

Lamb, R. C., Smalley, P. C. & Field, D. (1986). *P–T* condition for the Arendal granulites, southern Norway; implications for the roles of *P*, *T*, and $CO_2$ in deep crustal LILE-depletion. *Journal of Metamorphic Geology* **4**, 143–160.

Le Breton, N. & Thompson, A. B. (1988). Fluid-absent (dehydration) melting of biotite in metapelites in the early stages of crustal anatexis. *Contributions to Mineralogy and Petrology* **99**, 226–237.

Mattioli, G. S. & Bishop, F. C. (1984). Experimental investigation of the chromium–aluminum mixing parameter in garnet. *Geochimica et Cosmochimica Acta* **48**, 1367–1371.

Montel, J. M. & Vielzeuf, D. (1997). Partial melting of metagreywackes, Part 2. Compositions of minerals and melts. *Contributions to Mineralogy and Petrology* **128**, 176–196.

Newton, R. C., Aranovich, L. Ya., Hansen, E. C. & Vandenheuvel, B. A. (1998). Hypersaline fluids in Precambrian deep-crustal metamorphism. *Precambrian Research* **91**, 41–63.

Paktunc, A. D. & Baer, A. J. (1986). Geothermobarometry of the northwestern margin of the Superior Province: implications for its tectonic evolution. *Journal of Geology* **94**, 381–394.

Pan, Y., Fleet, M. E. & Williams, H. R. (1994). Granulite-facies metamorphism in the Quetico Subprovince, north of Manitouwadge, Ontario. *Canadian Journal of Earth Sciences* **31**, 1427–1439.

Patiño Douce, A. E. (1993). Titanium substitution in biotite: an empirical model with applications to thermometry, $O_2$ and $H_2O$ barometries, and consequences for biotite stability. *Chemical Geology* **108**, 133–162.

Patiño Douce, A. E. & Beard, J. S. (1994). $H_2O$ loss from hydrous melts during fluid-absent piston-cylinder experiments. *American Mineralogist* **79**, 585–588.

Patiño Douce, A. E. & Beard, J. S. (1995). Dehydration-melting of biotite gneiss and quartz amphibolite from 3 to 15 kbar. *Journal of Petrology* **36**, 707–738.

Patiño Douce, A. E. & Beard, J. S. (1996). Effects of *P*, $f(O_2)$ and Mg/Fe ratio on dehydration melting of model metagreywackes. *Journal of Petrology* **37**, 999–1024.

Patiño Douce, A. E. & Harris, N. (1998). Experimental constraints on Himalayan anatexis. *Journal of Petrology* **39**, 689–710.

Patiño Douce, A. E. & Johnston, A. D. (1991). Phase equilibria and melt productivity in the pelitic system: implications for the origin of peraluminous granitoids and aluminous granulites. *Contributions to Mineralogy and Petrology* **107**, 202–218.

Patiño Douce, A. E., Humphreys, E. D. & Johnston, A. D. (1990). Anatexis and metamorphism in tectonically thickened continental crust exemplified by the Sevier hinterland, western North America. *Earth and Planetary Science Letters* **97**, 290–315.

Percival, J. A. (1983). High-grade metamorphism in the Chapleau–Foleyet Area, Ontario. *American Mineralogist* **68**, 667–686.

Peterson, J. W. & Newton, R. C. (1989). $CO_2$-enhanced melting of biotite-bearing rocks at deep-crustal pressure–temperature conditions. *Nature* **340**, 378–380.

Peterson, J. W., Chacko, T. & Kuehner, S. M. (1991). The effects of fluorine on the vapor-absent melting of phlogopite + quartz: implications for deep crustal processes. *American Mineralogist* **76**, 470–476.

Phillips, G. N. & Wall, V. J. (1981). Evaluation of prograde regional metamorphic conditions, their implications for the heat source and

water activity during metamorphism in the Willyama Complex, Broken Hill, Australia. *Bulletin de Minéralogie* **104**, 801–810.

Pickering, J. M. & Johnston, A. D. (1998). Fluid-absent melting behavior of a two-mica metapelite: experimental constraints on the origin of Black Hills granite. *Journal of Petrology* **39**, 1788–1804.

Ravindra Kumar, G. R. & Chacko, T. (1986). Mechanisms of charnockite formation and break down in Southern Kerala: implications for the origin of the South Indian granulite terrain. *Journal of the Geological Society of India* **28**, 277–288.

Ravindra Kumar, G. R., Srikantappa, C. & Hansen, E. C. (1985). Charnockite formation at Ponmudi in southern Kerala. *Nature* **313**, 207–209.

Sack, R. O. & Ghiorso, M. S. (1989). Importance of considerations of mixing properties in establishing an internally consistent thermodynamic database: thermochemistry of minerals in the system $Mg_2SiO_4$–$Fe_2SiO_4$–$SiO_2$. *Contributions to Mineralogy and Petrology* **102**, 41–68.

Santosh, M. & Yoshida, M. (1992). A petrologic and fluid inclusion study of charnockites from the Lutzow–Holm Bay region, East Antarctica: evidence for fluid-rich metamorphism in the lower-crust. *Lithos* **29**, 107–126.

Schreurs, J. (1985). Prograde metamorphism of metapelites, garnet–biotite thermometry and prograde changes of biotite chemistry in high-grade rocks of West Uusimaa, southwest Finland. *Lithos* **18**, 69–80.

Skjerlie, K. P. & Johnston, A. D. (1993). Vapor-absent melting at 10 kbar of biotite- and amphibole-bearing tonalitic gneiss: implication for the generation of A-type granites. *Geology* **20**, 263–266.

Skjerlie, K. P., Patiño Douce, A. E. & Johnston, A. D. (1993). Fluid-absent melting of a layered crustal protolith: implications for the generation of anatectic granites. *Contributions to Mineralogy and Petrology* **114**, 365–378.

Spear, F. S. & Florence, F. P. (1992). Thermobarometry in granulites: pitfalls and new approaches. *Precambrian Research* **55**, 209–241.

Srikantappa, C., Raith, M. & Spiering, B. (1985). Progressive charnockitisation of a leptynite–khondalite suite in southern Kerala, India—evidence for formation of the charnockites through decrease in fluid pressure? *Journal of the Geological Society of India* **26**, 849–872.

Stevens, G., Clemens, J. D. & Droop, G. T. R. (1997). Melt production during granulite-facies anatexis: experimental data from 'primitive' metasedimentary protoliths. *Contributions to Mineralogy and Petrology* **128**, 352–370.

Trønnes, R. G., Edgar, A. D. & Arima, M. (1985). A high pressure–high temperature study of $TiO_2$ solubility in Mg-rich phlogopite: implications to phlogopite chemistry. *Geochimica et Cosmochimica Acta* **49**, 2323–2329.

Vielzeuf, D. & Montel, J. M. (1994). Partial melting of metagreywackes. 1. Fluid-absent experiments and phase relationships. *Contributions to Mineralogy and Petrology* **117**, 375–393.

Vielzeuf, D. & Holloway, J. R. (1988). Experimental determination of the fluid-absent melting relations in the pelitic system. Consequences for crustal differentiation. *Contributions to Mineralogy and Petrology* **98**, 257–276.

Waters, D. J. (1988). Partial melting and the formation of granulite facies assemblages in Namaqualand, South Africa. *Journal of Metamorphic Geology* **6**, 387–404.

Windom, K. E. & Boettcher, A. L. (1976). The effect of reduced activity of anorthite on the reaction grossular + quartz = anorthite + wollastonite: a model for plagioclase in the earth's lower crust and upper mantle. *American Mineralogist* **61**, 889–896.

Young, D. A. (1995). Kornerupine-group minerals in Grenville granulite-facies paragneiss, Reading Prong, New Jersey. *Canadian Mineralogist* **33**, 1255–1262.